Article

Length Dependence of the Coil # β-Sheet Transition in a Membrane Environment

Matthias Meier, and Joachim Seelig

J. Am. Chem. Soc., **2008**, 130 (3), 1017-1024 • DOI: 10.1021/ja077231r

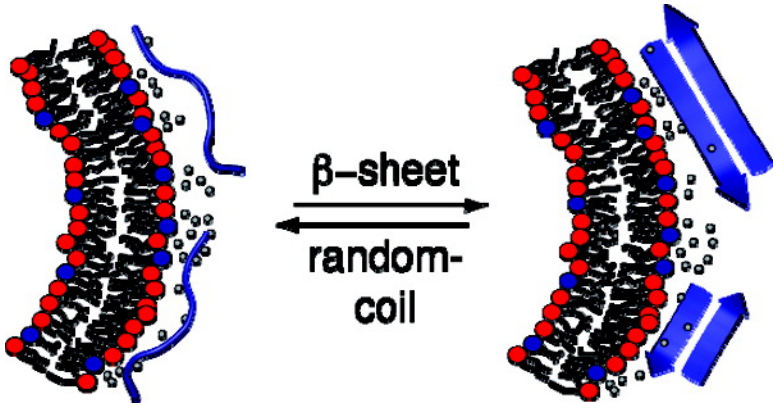

More About This Article

Additional resources and features associated with this article are available within the HTML version:

- Supporting Information
- Access to high resolution figures
- Links to articles and content related to this article
- Copyright permission to reproduce figures and/or text from this article

View the Full Text HTML

J|A|C|S
ARTICLES
Published on Web 12/29/2007

Length Dependence of the Coil ⇆ β-Sheet Transition in a Membrane Environment

Matthias Meier and Joachim Seelig*

Department of Biophysical Chemistry, Biozentrum, University of Basel, Klingelbergstrasse 50/70, CH-4056 Basel, Switzerland

Received September 18, 2007; E-mail: joachim.seelig@unibas.ch

Abstract: The most abundant structural element in protein aggregates is the β-sheet. Designed peptides that fold into a β-sheet structure upon binding to lipid membranes are useful models to elucidate the thermodynamic characteristics of the random coil ⇆ β-structure transition. Here, we examine the effect of strand length on the random coil ⇆ β-sheet transition of the $(KIGAKI)_n$ peptide with the total chain length varying between 7 and 30 amino acids. The β-sheet content of the peptides in the presence and absence of membranes was measured with circular dichroism spectroscopy. The peptides were titrated with small unilamellar lipid vesicles, and the thermodynamic binding parameters were determined with isothermal titration calorimetry (ITC). Membrane binding includes at least two processes, namely (i) the transfer of the peptide from the aqueous phase to the lipid surface and (ii) the conformational change from a random coil conformation to a β-sheet structure. CD spectroscopy and ITC analysis demonstrate that β-sheet formation depends cooperatively on the peptide chain length with a distinct increase in β-structure for $n > 10-12$. Binding to the lipid membrane is an entropy-driven process as the binding enthalpy is always endothermic. The contribution of the β-sheet folding reaction to the overall process was determined with analogues of the KIGAKI repeat where two adjacent amino acids were replaced by their D-enantiomers. The folding reaction for peptides with $n \geq 12$ is characterized by a negative free folding energy of $\Delta G^\circ_\beta \cong -0.15$ kcal/mol per amino acid residue. The folding step proper is exothermic with $\Delta H^\circ_\beta \cong -0.2$ to -0.6 kcal/mol per residue and counteracted by a negative entropy term $T\Delta S^\circ_\beta = -0.1$ to -0.5 kcal/mol per residue, depending on the chain length ($18 \leq n \leq 30$). For a short chain with $n = 12$, β-sheet formation is unfavorable with $\Delta G^\circ_\beta \sim +0.08$ kcal/mol per residue. Small changes of environmental parameters like pH or temperature can thus be anticipated to have profound effects on aggregation reactions, leading to amyloid fibril formation.

Introduction

β-Sheet folds in proteins are typically 2 to 6 residues in length, with few longer than 12 residues.[1,2] In comparison to α-helices which, on the average, have 7−20 residues,[3,4] β-sheet structures tend to be distinctively shorter. Interestingly, current models of β-sheets in non-native protein structures, i.e., amyloid fibrils, are about 10−15 residues in length.[5−7] Length stabilization is well-known for the α-helix[8,9] but is still controversial for the β-sheet structure. Isolated helices become more stable as the length of the α-helix increases. However, a more complex situation is encountered in the case of β-sheets since two orthogonal dimensions must be considered for β-sheet stabilization,[10] namely parallel and perpendicular to the strands. A closer insight into stabilization forces of β-sheets is obtained from small model peptides forming a β-hairpin which can be considered as equivalent to a two-stranded antiparallel β-sheet.[7,10] In such model peptides the length dependence of the β-sheet stability has been examined in both dimensions. Extension of the β-sheet structure perpendicular to the strand has been shown to gradually stabilize the β-sheet,[11−13] whereas a discontinuous effect was found upon strand lengthening along the peptide axis. It has been suggested that β-sheet stability may not increase beyond seven to nine residues.[14]

The thermodynamic analysis of β-sheet formation in aqueous solution is hampered by the low solubility of the corresponding peptides. Chain extension usually reduces the solubility even further. β-Sheet formation and peptide solubility are, however,

(1) Kabsch, W.; Sander, C. *Biopolymers* **1983**, *22*, 2577−2637.
(2) Penel, S.; Morrison, R. G.; Dobson, P. D.; Mortishire-Smith, R. J.; Doig, A. *J. Protein Eng.* **2003**, *16*, 957−961.
(3) Barlow, D. J.; Thornton, J. M. *J. Mol. Biol.* **1988**, *201*, 601−619.
(4) Kumar, S.; Bansal, M. *Biophys. J.* **1998**, *75*, 1935−1944.
(5) Jaroniec, C. P.; MacPhee, C. E.; Bajaj, V. S.; McMahon, M. T.; Dobson, C. M.; Griffin, R. G. *Proc. Natl. Acad. Sci. U.S.A.* **2004**, *101*, 711−716.
(6) Petkova, A. T.; Ishii, Y.; Balbach, J. J.; Antzutkin, O. N.; Leapman, R. D.; Delaglio, F.; Tycko, R. *Proc. Natl. Acad. Sci. U.S.A.* **2002**, *99*, 16742−16747.
(7) Chan, J. C.; Oyler, N. A.; Yau, W. M.; Tycko, R. *Biochemistry* **2005**, *44*, 10669−10680.
(8) Zimm, B. H.; Doty, P.; Iso, K. *Proc. Natl. Acad. Sci. U.S.A.* **1959**, *45*, 1601−1607.
(9) Scholtz, J. M.; Qian, H.; York, E. J.; Stewart, J. M.; Baldwin, R. L. *Biopolymers* **1991**, *31*, 1463- 1470.
(10) Gellman, S. H. *Curr. Opin. Chem. Biol.* **1998**, *2*, 717−725.
(11) Syud, F. A.; Stanger, H. E.; Mortell, H. S.; Espinosa, J. F.; Fisk, J. D.; Fry, C. G.; Gellman, S. H. *J. Mol. Biol.* **2003**, *326*, 553−568.
(12) Sharman, G. J.; Searle, M. S. *J. Am. Chem. Soc.* **1998**, *120*, 5291−5300.
(13) Searle, M. S.; Williams, D. H.; Packman, L. C. *Nat. Struct. Biol.* **1995**, *2*, 999−1006.
(14) Stanger, H. E.; Syud, F. A.; Espinosa, J. F.; Giriat, I.; Muir, T.; Gellman, S. H. *Proc. Natl. Acad. Sci. U.S.A.* **2001**, *98*, 12015−12020.

increased in hydrophobic environments such as organic solvents and lipid membranes.[15] A case in point are the Alzheimer peptides (Aβ). The typical chain length of these peptides is 40 to 42 amino acids, and their solubility limit as monomers is $\sim$10 μM in 10 mM NaCl solution.[16−21] Aβ(1−40) displays a random coil $\leftrightarrows$ β-sheet transition in solution upon increasing the peptide concentration. The same transition can also be induced upon addition of negatively charged lipid vesicles to an Aβ solution of constant Aβ concentration.[22,23]

Few systematic studies on the stabilization of a β-sheet structure in a membrane environment are available to date. We have recently determined the thermodynamic parameters of the membrane-induced random coil $\leftrightarrows$ β-sheet folding reaction of the $(KIGAKI)_3$ peptide using isothermal titration calorimetry (ITC).[24] The $(KIGAKI)_3NH_2$ peptide has no amphipathic character as an α-helix but can form a highly amphipathic β-sheet when bound to lipid bilayers.[25] ITC data were obtained for the binding of the $(KIGAKI)_3$ peptide to anionic lipid vesicles. The thermodynamic parameters are the result of two different processes, namely, (i) the transfer of the peptide from the aqueous phase to the lipid surface and (ii) the conformational change of the peptide from a random coil conformation to a β-sheet structure. The contribution of the folding reaction to the overall process was elucidated with analogues of the KIGAKI repeat, in which two adjacent amino acids were replaced by their D-enantiomers. Substitution of L-amino acids by their D-enantiomers led to a local disturbance of the β-sheet structure,[26,27] the extent of which was dependent on the number and the position of the D-amino acid substitutions. β-Sheet formation on the surface of negatively charged membranes was quantitated with circular dichroism (CD) spectroscopy. By correlating the thermodynamic parameters with the percentage of β-sheet formation for peptides with and without D-amino acid substitution, it was possible to separate the binding thermodynamics from the process of β-sheet formation.[24]

In the present study we were interested in the influence of the peptide chain length on the thermodynamic parameters of β-sheet formation. To this purpose, we increased the length of the $(KIGAKI)_3$ peptide by one or two KIGAKI repeats or we shortened the peptide to 12, 10, 8, or 7 amino acid residues. The thermodynamic binding parameters and structural changes of all peptides were determined with ITC and circular dichroism spectroscopy, respectively. Distinct differences were observed between short ($n \leq 12$) and long peptides ($18 \leq n \leq 30$). D-Amino acid substitutions were introduced for short ($n = 12$) and long ($n = 24$) peptides to separate the conformational change from membrane binding.

Table 1. Amino Acid Sequences of the Synthesized Peptides[a]

short-hand notation used in the text	peptide sequence
pep-7	KWGAKI-K-NH_2
pep-8	KWGAKI-KI-NH_2
pep-10	KWGAKI-KIGA-NH_2
pep-12	KWGAKI-KIGAKI-NH_2
pep-18[b]	KWGAKI-$(KIGAKI)_2$-NH_2
pep-24	KWGAKI-$(KIGAKI)_3$-NH_2
pep-30	KWGAKI-$(KIGAKI)_4$-NH_2
pep-12-1DD	KWG*ak*I-KIGAKI-NH_2
pep-12-2DD	KWG*ak*I-KIG*ak*I-NH_2
pep-24-2DD	KWGAKI-KIG*ak*I-KIG*ak*I-KIGAKI-NH_2
pep-24-3DD	KWGAKI-KIG*ak*I-KIG*ak*I-KIG*ak*I−NH_2

[a] The italicized small letters in the peptide sequences denote D amino acids. The first number of the short hand notation represents the peptide length, and the second, the number of double D amino acid substitutions. [b] Data were taken from ref 24.

Results

Membrane Binding Equilibrium of $(KIGAKI)_n$ Repeats Measured with Isothermal Titration Calorimetry. Table 1 shows the set of synthesized peptides with their corresponding short-hand notation. For accurate determination of the peptide concentration, Ile-2 was replaced by Trp, and peptide concentrations were calculated using the Trp molar extinction coefficients (5500 M^{-1} cm^{-1}). The C-terminal carboxyl groups of all peptides were amidated.

In the following the term "binding" is used in a general sense to describe the adsorption of the cationic peptide from the bulk solution to the anionic membrane surface. Binding of the KIGAKI peptides with a length of 7 to 30 residues to negatively charged lipid vesicles was studied by ITC. Following the standard protocol for lipid-into-peptide titration,[28] a diluted peptide solution was filled into the calorimeter cell and 10 μL aliquots of a lipid suspension were injected at constant time intervals. Figure 1A shows a representative calorimetric trace obtained at 25 °C by titration of 50 μM pep-8 with 25 mM SUVs composed of POPE/POPG/mPEG 2000 POPE (70:25:5 molar ratio).

Each lipid injection causes an endothermic reaction as illustrated by the calorimetric trace. The size of the titration peak becomes smaller with an increasing number of injections as less peptide is available for binding. After about 20 injections all peptide is bound and further lipid injections entail no additional heat of reaction (except of dilution effects). The molar binding enthalpy, $\Delta H°$, can then be calculated according to

$$\Delta H° = \sum_{i=1}^{n} h_i / n°_{pep} \qquad (1)$$

where $n°_{pep}$ is the total molar amount of peptide in the calorimeter cell and $\sum_{i=1}^{n} h_i$ is the cumulative heat of reaction. The measured binding enthalpies for all peptides except for pep-7 are summarized in Table 2. For pep-7 we observed only small heat peaks upon titration with anionic lipid vesicles.

(15) Sharman, G. J.; Searle, M. S. *J. Am. Chem. Soc.* **1998**, *120*, 5291−5300.
(16) Harper, J. D.; Lansbury, P. T., Jr. *Annu. Rev. Biochem.* **1997**, *66*, 385−407.
(17) Williams, A. D.; Shivaprasad, S.; Wetzel, R. *J. Mol. Biol.* **2006**, *357*, 1283−1294.
(18) Hortschansky, P.; Christopeit, T.; Schroeckh, V.; Fandrich, M. *Protein Sci.* **2005**, *14*, 2915−2918.
(19) Hortschansky, P.; Schroeckh, V.; Christopeit, T.; Zandomeneghi, G.; Fandrich, M. *Protein Sci.* **2005**, *14*, 1753−1759.
(20) Sengupta, P.; Garai, K.; Sahoo, B.; Shi, Y.; Callaway, D. J.; Maiti, S. *Biochemistry* **2003**, *42*, 10506−10513.
(21) Gorman, P. M.; Yip, C. M.; Fraser, P. E.; Chakrabartty, A. *J. Mol. Biol.* **2003**, *325*, 743−757.
(22) Terzi, E.; Holzemann, G.; Seelig, J. *J. Mol. Biol.* **1995**, *252*, 633−642.
(23) Terzi, E.; Holzemann, G.; Seelig, J. *Biochemistry* **1997**, *36*, 14845−14852.
(24) Meier, M.; Seelig, J. *J. Mol. Biol.* **2007**, *369*, 277−289.
(25) Blazyk, J.; Wiegand, R.; Klein, J.; Hammer, J.; Epand, R. M.; Epand, R. F.; Maloy, W. L.; Kari, U. P. *J. Biol. Chem.* **2001**, *276*, 27899−27906.
(26) Rothemund, S.; Beyermann, M.; Krause, E.; Krause, G.; Bienert, M.; Hodges, R. S.; Sykes, B. D.; Sonnichsen, F. D. *Biochemistry* **1995**, *34*, 12954−12962.
(27) Wieprecht, T.; Dathe, M.; Schumann, M.; Krause, E.; Beyermann, M.; Bienert, M. *Biochemistry* **1996**, *35*, 10844−10853.
(28) Seelig, J. *Biochim. Biophys. Acta* **1997**, *1331*, 103−116.

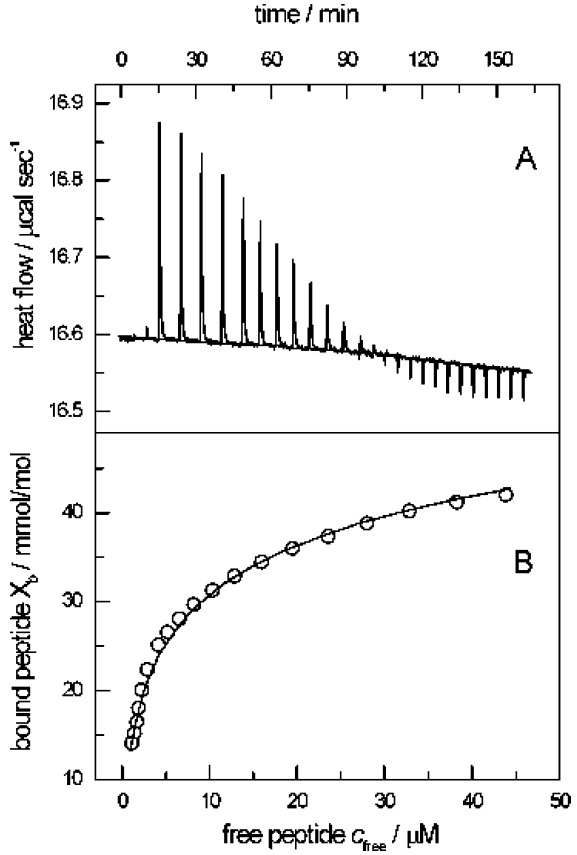

Figure 1. (A) Calorimetric trace obtained by titrating small unilamellar vesicles (25 mM; POPE/POPG/mPEG 2000 POPE (70:25:5 mol/mol/mol)) into a 50 μM pep-8 solution. Both in buffer (25 mM Tris, 50 mM NaCl, pH 7.4, 25 °C). The injection volume of the lipid vesicles was 10 μL; injections occurred at 5 min intervals. (B) Binding isotherm of pep-8 derived from the ITC experiment shown in A. The extent of bound peptide per lipid (lipid of outer monolayer only) is plotted vs the equilibrium concentration of free peptide in solution. The solid line is the theoretical binding isotherm derived by combining the Gouy−Chapman theory with a surface partition equilibrium.

Table 2. Thermodynamic Parameters for the Binding of KIGAKI Peptides to POPE/POPG/mPEG 2000 PE (70:25:5 Molar Ratio) SUVs at 25 °C

peptide	K_0 (M^{-1})	$\Delta H°$ (kcal/mol)	$T\Delta S°$ [a] (kcal/mol)	$\Delta G°$ [b] (kcal/mol)	z_{eff}	ΔC_p cal/mol K
pep-7	no ITC data at 25 °C					
pep-8	170 ± 40	1.3 ± 0.1	6.7	−5.4 ± 0.2	3.2	
pep-10	80 ± 20	2.7 ± 0.1	7.6	−5.0 ± 0.15	3.2	
pep-12	55 ± 10	3.6 ± 0.3	8.3	−4.7 ± 0.15	3.7	−157
pep-18[c]	890 ± 150	6.3 ± 0.3	12.7	−6.4 ± 0.2	3.4	−84
pep-24	1200 ± 200	6.4 ± 0.3	12.6	−6.6 ± 0.2	3.7	−192
pep-30	2000 ± 400	5.2 ± 0.3	12.1	−6.9 ± 0.25	3.5	
pep-12-1DD	100 ± 20	3.35 ± 0.1	8.4	−5.1 ± 0.2	2.7	−141
pep-12-2DD	85 ± 10	3.0 ± 0.1	8.0	−5.0 ± 0.2	4.1	−134
pep-24-2DD	160 ± 30	9.8 ± 0.5	15.2	−5.4 ± 0.15	5.8	−325
pep-24-3DD	50 ± 40	10.9 ± 0.5	15.6	−4.68 ± 0.4	5.5	−411

[a] The entropy of the peptide binding reaction was calculated according to $\Delta G° = \Delta H° - T\Delta S°$. [b] The free energy of the peptide binding reaction was calculated according to $\Delta G° = -RT \ln(K_0 * 55.5)$. [c] Data taken from ref 24.

The ITC data can be translated into binding isotherms as described elsewhere.[29] Figure 1B shows the binding isotherm corresponding to the ITC measurement of Figure 1A. The binding isotherm, $X_b = f(c_f)$, describes the extent of binding, X_b, as a function of the equilibrium concentration of the free peptide c_f. X_b is defined as $X_b^{(i)} = n_{pep,bound}^{(i)}/n_L^{(i)}$, where $n_{pep,bound}^{(i)}$ is the molar amount of bound peptide after i injections and $n_L^{(i)}$ is the molar amount of injected lipid available for binding. $n_L^{(i)}$ is given by the lipid concentration in the injection syringe and the number of injections i. In the present case the charged peptides are not able to translocate across the membrane and only the outer membrane leaflet of the SUVs (60% of the total lipid) is available for peptide binding. $n_{pep,bound}^{(i)}$ can be calculated from the experimental heats of reaction, h_i, according to

$$n_{p,\,bound}^{(i)} = \sum_{k=1}^{i} h_k/(\Delta H° \, V_{Cell} \, c_{0,pep}) \qquad (2)$$

$c_{0,pep}$ is the total peptide concentration in the calorimeter cell. Knowledge of the amount of bound peptide allows the calculation of the peptide concentration free in solution from mass conservation. The binding isotherm can thus be determined in a model-independent fashion.

Further analysis of the binding isotherm is based on a *surface partitioning model*, in which the peptide adsorption is related to the peptide concentration c_M found immediately above the plane of binding[27,30]

$$X_b = K_0 \, c_M \qquad (3)$$

The model is based on the observation that the negatively charged membrane surface will attract cationic species in its vicinity. The peptide concentration will thus increase from its equilibrium value, c_f, far away from the membrane surface to the much higher value c_M in the lipid−water interface. The electrostatic equilibrium is governed by the Boltzmann relation

$$c_M = c_f \exp(-z_{pep}F_0\psi/RT) \qquad (4)$$

where z_{pep} is the effective peptide charge (usually smaller than the nominal charge), ψ is the membrane surface potential, F_0 is the Faraday constant, and RT is the thermal energy. Using the Gouy−Chapman theory it is possible to calculate the surface potential ψ and the surface concentration c_M for each data point of the binding isotherm leading to a surface partition constant K_0.[31,32] A detailed description of this binding model has been given elsewhere.[29] As an additional feature the binding of Na^+ ions to phosphatidylglycerol was taken into account with a Langmuir adsorption isotherm and a Na^+ binding constant of 0.6 M^{-1}.[33] Tris/HCl buffer was counted as a 1−1 salt. The continuous line in Figure 1B is the best theoretical fit to the experimental data. The effective peptide charge is $z_{pep} = 3.1-3.3$, and the surface potential varies between $\psi = -45$ mV at low X_b to $\psi = -17$ mV at the highest X_b value. The binding constant according to eq 4 is $K_0 = 170$ M^{-1}. Excellent agreement between the model and the experimental data is obtained for all peptides. The corresponding binding constants K_0 are listed in Table 2. The free energy of binding, $\Delta G°$, follows from

(29) Seelig, J.; Nebel, S.; Ganz, P.; Bruns, C. *Biochemistry* **1993**, *32*, 9714−9721.
(30) Wenk, M. R.; Seelig, J. *Biophys. J.* **1997**, *73*, 2565−2574.
(31) McLaughlin, S. *Curr. Top. Membr. Transp.* **1977**, 71−144.
(32) Aveyard, R.; Haydon, D. A. *Cambridge Chemistry Tests: An Introduction to the Principles of Surface Chemistry*, 1973.
(33) Eisenberg, M.; Gresalfi, T.; Riccio, T.; McLaughlin, S. *Biochemistry* **1979**, *18*, 5213−5223.

$$\Delta G^\circ = -RT \ln(55.5\, K_0) \qquad (5)$$

where the factor 55.5 is the molar concentration of water and corrects for the cratic contribution. The binding entropy can then be calculated from $\Delta G^\circ = \Delta H^\circ - T\Delta S^\circ$.

Circular Dichroism Spectroscopy of KIGAKI Peptides with and without Lipid. The CD spectra of KIGAKI peptides of chain length $n = 8$ to 30 in buffer are displayed in Figure 2A. All spectra are characteristic of a predominantly random coil conformation. The ellipticity decreases with decreasing peptide length, and the spectra can be simulated with conventional CD simulation programs. The random coil content is in the range 71 to 85% while the contribution of β-structure is 15 to 30%. The detailed analysis is given in Table 3.

Upon addition of anionic lipid vesicles the cationic peptides bind to the membrane surface and undergo a conformational change to a β-structured conformation. Figure 2B displays the corresponding CD spectra recorded in an excess of anionic lipid vesicles. The β-sheet content increases from 46% for $n = 8$ to 90−100% for $n = 18$, 24, and 30. The detailed analysis is again listed in Table 3. We have also synthesized peptides with a chain length of six and seven residues. They bind only weakly, and the changes in the CD spectra are small.

The last two columns in Table 3 quantitate the observed spectral change in terms of the fraction of β-structure, Δf_β, and the total number of amino acids, $\Delta\beta$(aa) involved in the random coil ⇆ β-structure transition. $\Delta\beta$(aa) is obtained by multiplying Δf_β with the peptide chain length n (= number of amino acids).

In Figure 3A the fractional change in β-structure, Δf_β, is plotted versus the chain length, n, revealing a cooperative dependence on n. The β-structure formation is small for $n \leq 10$ but increases sharply for longer peptides. Δf_β reaches a limiting value of about 0.85. Figure 3B shows the corresponding plot for the number of amino acid residues, $\Delta\beta$(aa), changing from random coil to β-structure. For $n \geq 12$ a straight line ($\Delta\beta$-(aa) = $1.03n - 5.5$) is obtained, suggesting that a minimum of six amino acids is required before a change in β-structure can be observed. As the slope is close to unity, any lengthening of the chain produces only β-structured segments. It further follows from Table 3 that a plot of Δf_β vs Δf_{rc} yields a straight line passing through the origin with slope $m = -1$ (not shown). The increase in β-structure occurs completely at the expense of random coil domains.

We may now relate the observed structural changes with the thermodynamic binding data (Table 2). In Figure 4 the thermodynamic parameters ΔH°, ΔG°, and $T\Delta S^\circ$ are plotted against $\Delta\beta$(aa), revealing two distinct binding regions. For short chains ($n_{total} \leq 12$) $\Delta\beta$(aa) is small and all three thermodynamic parameters vary with a positive slope; for long chains $\Delta\beta$(aa) is large and the slopes become negative. Figure 4 also demonstrates that ΔH° and $T\Delta S^\circ$ are both positive and vary almost in parallel over the whole range of $\Delta\beta$(aa) investigated. The Gibbs free energy, ΔG°, is thus the difference of two large numbers displaying a much smaller variation with $\Delta\beta$(aa).

Binding versus β-Structure Formation. KIGAKI Peptides with D-Enantiomers. The thermodynamic parameters measured in the ITC experiments are composed of the binding to the lipid membrane and the conformational change induced by this interaction. The experiments described so far allow no separation of the two effects as membrane binding (without a conformational change) may vary with the peptide chain length. We have therefore synthesized peptides with a given chain length (n = 12 or 24) in which pairs of L-amino acids where replaced by their D-amino acids (cf. Table 1). This substitution reduces the potential of the peptides to form β-structures. It is assumed that the basic binding properties of a given all-L peptide and its D,D analogues are identical and that the variation of the thermody-

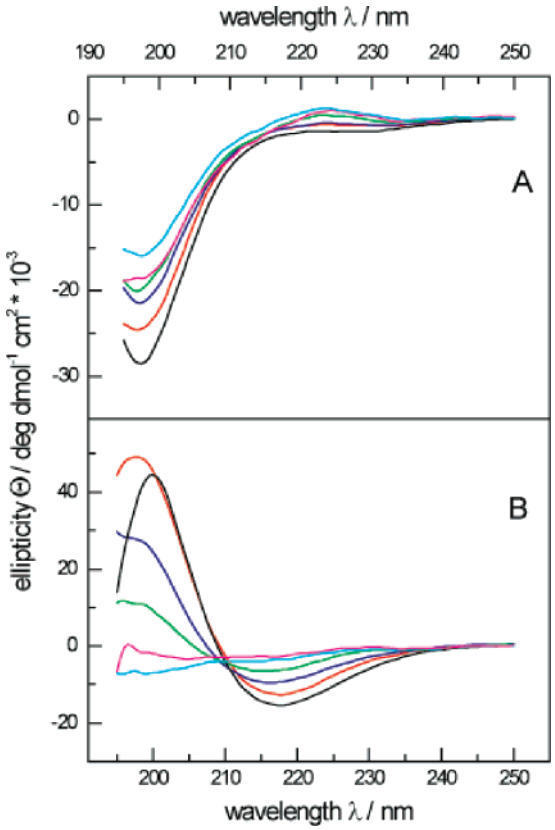

Figure 2. Circular dichroism spectra of KIGAKI peptides of different chain lengths recorded (A) in buffer solution and (B) with an excess of POPE/POPG/mPEG 2000 POPE (45:50:5) SUVs (L/P = 15). The CD spectra correspond to a chain length of n = 30, 24, 18, 12, 8, and 10 (from bottom to top) at 198 nm in (A) or 217 nm in (B). The spectra were recorded at peptide concentrations of 50−75 μM in 5 mM cacodylate buffer (pH 7.4).

Table 3. CD Spectra Analysis of KIGAKI Peptides with and without Double D-Amino Acid Substitution in Aqueous Solution and with Excess Lipid

		CD spectra in aqueous solution			CD spectra with excess lipids			change of β-structure	
peptide	% D-amino acids[a]	f_{rc}	f_β [b]	f_α	f_{rc}	f_β	f_α	Δf_β [c]	$\Delta\beta$(aa)[d]
Pep-8		0.71	0.29	0	0.54	0.46	0	0.17	1.4
Pep-10		0.70	0.30	0	0.48	0.52	0	0.22	2.2
Pep-12		0.75	0.25	0	0.21	0.79	0	0.54	6.5
Pep-18[e]		0.77	0.23	0	0.02	0.98	0	0.75	13.5
Pep-24		0.81	0.16	0.03	0	0.99	0.01	0.83	20
Pep-30		0.85	0.03	0.12	0	0.95	0.05	0.85[f]	25.5
Pep-12-1DD	16.7	0.68	0.32	0	0.33	0.67	0	0.35	4.2
Pep-12-2DD	33	0.59	0.41	0	0.31	0.69	0	0.28	3.4
Pep-24-2DD	17	0.74	0.23	0.03	0.25	0.74	0.01	0.51	12.2
Pep-24-3DD	25	0.73	0.24	0.03	0.36	0.62	0.02	0.38	9.1

[a] Percentage of D amino acids in the peptide. [b] The table summarizes the fractions f_i of amino acids with conformation i. f_β is the sum of β-sheet and β-turn. [c] $\Delta f_\beta = f_\beta$(lipid) − f_β(buffer). [d] $\Delta\beta$(aa) = $\Delta f_\beta \times n_{total}$. [e] Data taken from ref 24. [f] For Pep-30 the α-helix content changes from buffer to lipid. The loss in random coil segments is considered to be the minimum of new folded β-structure.

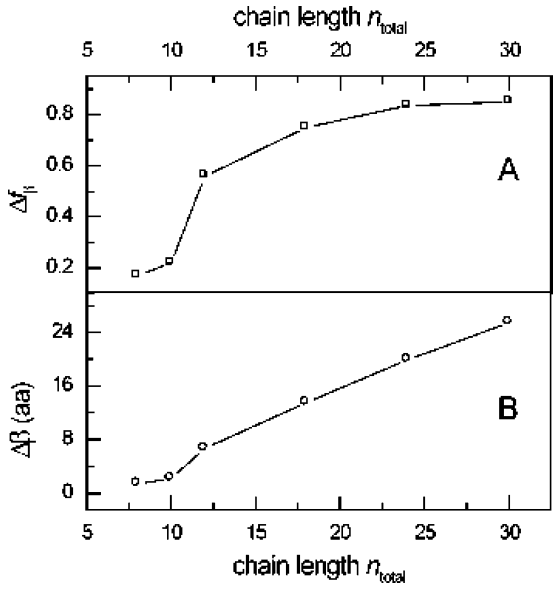

Figure 3. Membrane-induced β-structure. Binding of KIGAKI peptides to anionic lipid vesicles leads to an increase in β-structure which is measured with CD spectroscopy. f_β is the fraction of β-structure (β-sheet + β-turn) obtained from a simulation of the CD spectrum. Δf_β denotes the change in β-structure for a given peptide when moving from buffer to the lipid membrane. (A) Sigmoidal behavior of Δf_β as a function of chain length. (B) $\Delta\beta(\text{aa}) = \Delta f_\beta \times n_{total}$ as a function of the peptide chain length.

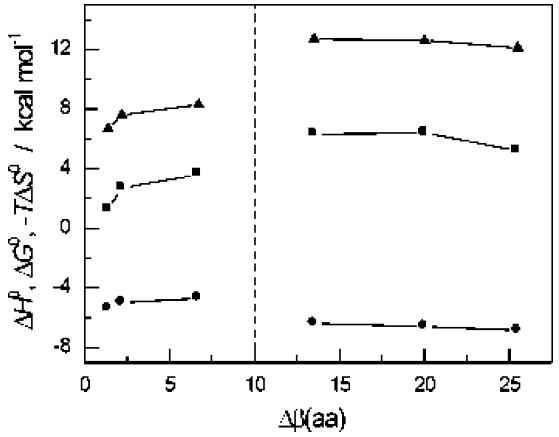

Figure 4. Thermodynamic parameters for the binding of $(KIGAKI)_n$ peptides to anionic membranes. The membrane composition and the experimental conditions are the same as those in Figure 1. The reaction enthalpy $\Delta H°$ (■), the reaction free energy $\Delta G°$ (●), and the entropy term $T\Delta S°$ (▲) are plotted as a function of the change in β-structure, $\Delta\beta$(aa).

namic parameters can be ascribed to different extents of β-sheet formation. Systematic D,D substitution at different chain positions has been successfully employed to quantitatively describe the membrane-induced α-*helix formation* of the antibacterial peptide magainin[34] and a mitochondrial signal peptide[35] and for the β-*structure formation* of pep-18.[24] In the present study we have extended this method to a longer $(KIGAKI)_4$ peptide (pep-24) with 2 or 3 D,D pairs and a shorter $(KIGAKI)_2$ peptide (pep-12) with 1 or 2 D,D pairs.

Figure 5 summarizes the CD spectra of pep-24 and its two analogues in buffer (Figure 5A) and in the presence of excess lipid (Figure 5B). The figure demonstrates a distinct change

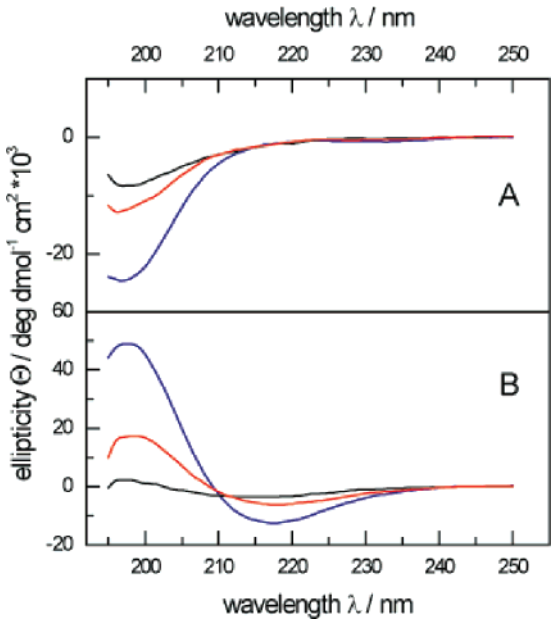

Figure 5. Circular dichroism spectra of pep-24 and two D,D analogues (A) in buffer and (B) in the presence of excess lipid. Spectra from bottom to top at 198 nm: (A) pep-24, pep-24-1DD, and pep-24-2DD and (B) pep-24-2DD, pep-24-1DD, and pep-24. The lipid vesicles (SUVs 30 nm) were composed of POPE/POPG/mPEG-2000 POPE in a molar ratio of 45:50:5. The lipid-to-peptide mol ratio was ~15. Spectra were recorded at peptide concentrations of 50−75 μM in 5 mM cacodylate buffer (pH 7.4).

from a random coil spectrum in buffer to a β-structured CD spectrum upon addition of lipids. It also reveals that the ellipticity is reduced as D-amino acids are incorporated into the sequence. An isosbestic point is observed at $\lambda = 210$ nm suggesting a two-state equilibrium. The evaluation of the CD spectra with D-amino acids has been described previously.[24] In short, we start with the peptide spectrum containing no D-amino acids which can be analyzed by the conventional CD simulation programs. The results are given in Table 3. Next, we reduce the ellipticities according to the fraction of D-amino acids in the analogue. If the fraction of D-amino acids in the sequence is X_D, the ellipticity of the all-L peptide in buffer or with lipid is multiplied by $(1-2X_D)$. In a third step, using the buffer and lipid spectra with corrected ellipticities, we generate linear combinations to reproduce the experimental spectra. The results of this conformational analysis are also listed in Table 3.

The structural changes as quantitated by $\Delta\beta$(aa) can then be correlated with the thermodynamic results. This is shown in Figure 6 for the three peptides with a chain length of $n = 12$, 18, and 24 residues and the three thermodynamic parameters $\Delta H°$, $\Delta G°$, and $T\Delta S°$. For each peptide a linear correlation is obtained between $\Delta\beta$(aa) and the thermodynamic parameters. Different slopes are, however, found for short and long peptides. For pep-12 the slopes of $\Delta H°$, $\Delta G°$, and $T\Delta S°$ are positive, and for pep-18 and pep-24 the slopes are negative. Table 4 summarizes the results of the linear regression analysis in terms of the intercepts ($\Delta H°_{bind}$, ΔG_{bind}, $T\Delta S°_{bind}$) and the slopes ($\Delta H°_\beta$, $\Delta G°_\beta$, $T\Delta S°_\beta$). The intercepts define hypothetical peptides which bind without a conformational change. The slopes, on the other hand, yield the contribution of a single amino acid residue to β-structure formation. Table 4 then demonstrates that both binding and folding are a function of the peptide chain length.

The analysis can be carried one step further by plotting the thermodynamic data of Table 4 against the peptide length *n*.

(34) Wieprecht, T.; Apostolov, O.; Beyermann, M.; Seelig, J. *J. Mol. Biol.* **1999**, *294*, 785−794.
(35) Wieprecht, T.; Apostolov, O.; Beyermann, M.; Seelig, J. *Biochemistry* **2000**, *39*, 15297−15305.

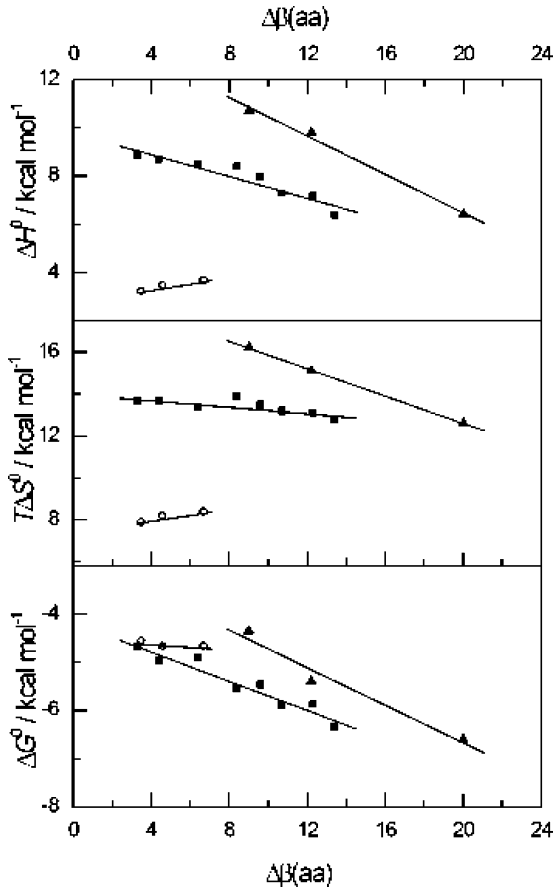

Figure 6. Thermodynamic binding parameters as a function of D,D substitution. (○) pep-12; (■) pep-18; (▲) pep-24. $\Delta\beta$(aa) denotes the number of amino acid residues which adopt β-structure when moving from the buffer to the membrane phase. For a given peptide, D,D substitutions lead to different $\Delta\beta$(aa) values. (A) Reaction enthalpies $\Delta H°$ as measured with ITC as a function of $\Delta\beta$(aa); (B) reaction entropy $T\Delta S°$; (C) Gibbs free energy $\Delta G°$. The thermodynamic parameters are experimental values which include the binding step proper and the peptide folding.

This is shown in Figure 7 for the binding (Figure 7A) and the folding parameters (Figure 7B). Inspection of Figure 7 shows for $n \geq 12$ that (i) all thermodynamic parameters are a linear function of the chain length, (ii) ΔH_i° and $T\Delta S_i^\circ$ (i = bind, fold) run almost parallel for binding and for folding, and (iii) as a consequence of the enthalpy−entropy compensation mechanism the Gibb's free energy, ΔG_i°, displays a much smaller variation than ΔH_i° and $T\Delta S_i^\circ$.

Figure 7B includes data for pep-30 for which no D,D substitutions were made. The corresponding analysis was performed as follows. The straight lines in Figure 7A were extrapolated to $n = 30$ and ΔH_{bind}°, ΔG_{bind}°, $T\Delta S_{bind}^\circ$ were obtained. Subtracting these data from the experimental results listed in Table 2 yields the contributions of the folding process. Dividing by the change in β-conformation of pep-30 ($\Delta\beta$(aa) = 12.85) yields the folding parameters per amino acid residue. Figure 7B demonstrates that the numbers fit well on the straight lines derived from D,D substitution for $n = 18$ and $n = 24$.

Specific Heat Capacities. Electrostatic as well as hydrophobic interactions contribute to membrane binding and peptide aggregation. In particular, the large positive entropic contribution to the binding reactions suggests a prominent role of the hydrophobic effect in the membrane binding reaction. The hallmark of the hydrophobic effect is a large reduction in the specific heat capacity, which is associated with the release of water from the hydrophobic surface. The last column in Table 2 shows measured heat capacities for selected peptides. The heat capacities are large and negative (−150 to −400 cal mol^{-1} K^{-1}) confirming the role of the hydrophobic effect in the binding process.

Discussion

The thermodynamic basis of β-sheet formation and the cooperativity of β-sheet folding are still open questions.[12,36] Stabilization energies of β-sheets appear to depend on the specific protein or peptide investigated, but it is generally believed that hydrophobic interactions are the dominant driving force for β-sheet folding in *aqueous* solution.[37,38] In particular, interactions between nonpolar side chains on adjacent strands were shown to stabilize β-sheet structure.[39−41] In contrast, in a *membrane environment* or in the interior of globular proteins, polar interactions and hydrogen bonds are assumed to drive β-sheet formation.[42,43]

In the present study we have addressed these questions with model peptides composed of KIGAKI repeats with chain length of $6 \leq n \leq 30$ and have studied their membrane-induced β-sheet formation. Membrane-binding requires an anionic surface and all membrane-bound peptides with a chain length $n \geq 7$ show an increase in β-structure compared to their conformation in solution. The β-content of the bound peptides as measured with CD spectroscopy is a function of the chain length and a plot of Δf_β vs n shows a sigmoidal increase with the midpoint at $n \sim 10-12$ (cf. Figure 3A). Peptides with a chain length $n > 10$ easily form β-structures, in shorter peptides the β-content is small. The steep transition between the two regions suggests a cooperative process.

^{2}H NMR studies with selectively deuterated pep-18 have shown that membrane-induced β-structure formation leads to large, immobile peptide aggregates at the membrane surface.[24] The molecular structure of the lipid bilayer remains largely unaffected by these aggregates. It is reasonable to assume a similar arrangement also for pep-24 and pep-30.

The thermodynamic measurements comprise both the binding of the peptides to the membrane surface and their folding to β-structure. Common to all peptides ($n = 8-30$) is the fact that the reaction enthalpy is endothermic and that the reaction is driven by entropy. The positive entropy contribution is unexpected as the formation of β-structure together with peptide immobilization and aggregation on the membrane surface lead to a better ordered system. On the other hand, the temperature dependence of $\Delta H°$ is characterized by a large negative heat capacity of $\Delta C_p^\circ = -150$ to -400 cal mol^{-1} K^{-1}, suggesting the release of hydration water. The binding of the $(KIGAKI)_n$ peptides to the anionic membrane is thus strongly influenced

(36) de Alba, E.; Jimenez, M. A.; Rico, M. *J. Am. Chem. Soc.* **1997**, *119*, 175−183.
(37) Chou, K. C.; Nemethy, G.; Scheraga, H. A. *J. Mol. Biol.* **1983**, *168*, 389−407.
(38) Smith, C. K.; Withka, J. M.; Regan, L. *Biochemistry* **1994**, *33*, 5510−5517.
(39) Espinosa, J. F.; Munoz, V.; Gellman, S. H. *J. Mol. Biol.* **2001**, *306*, 397−402.
(40) Ramirez-Alvarado, M.; Blanco, F. J.; Serrano, L. *Protein Sci.* **2001**, *10*, 1381−1392.
(41) Russell, S. J.; Blandl, T.; Skelton, N. J.; Cochran, A. G. *J. Am. Chem. Soc.* **2003**, *125*, 388−395.
(42) Wimley, W. C.; White, S. H. *Nat. Struct. Biol.* **1996**, *3*, 842−848.
(43) Roseman, M. A. *J. Mol. Biol.* **1988**, *201*, 621−623.

Table 4. Binding and Folding of $(KIGAKI)_n$ Peptides at the Membrane Surface (Thermodynamic Parameters for the Two Processes of Binding and Folding Only)

			intrinsic peptide binding			β-sheet folding		
	peptide length	$\Delta\beta$(aa)[a]	ΔH°_{bind} (kcal/mol)	$T\Delta S^\circ_{bind}$ (kcal/mol)	ΔG°_{bind} (kcal/mol)	ΔH°_{bind} (kcal/mol)	$T\Delta S^\circ_{bind}$ (kcal/mol)	ΔG°_{bind} (kcal/mol)
pep-12	12	6.7	2.7 ± 0.4	7.3 ± 0.3	-4.5 ± 0.2	0.13 ± 0.1	0.15 ± 0.1	0.03 ± 0.1
pep-18[b]	18	13.5	9.8 ± 0.3	14.1 ± 0.3	-4.2 ± 0.2	-0.23 ± 0.05	-0.1 ± 0.05	-0.15 ± 0.05
pep-24	24	20	14.5 ± 0.5	18.8 ± 0.3	-3.3 ± 0.2	-0.40 ± 0.05	-0.29 ± 0.05	-0.17 ± 0.05
pep-30	30	25.6	20.9[c]	24.9[c]	−2.5[c]	−0.6	−0.5	−0.12

[a] Number of amino acid residues which change to β-structure for the all-L-peptide. [b] Data taken from ref 24. [c] Extrapolated.

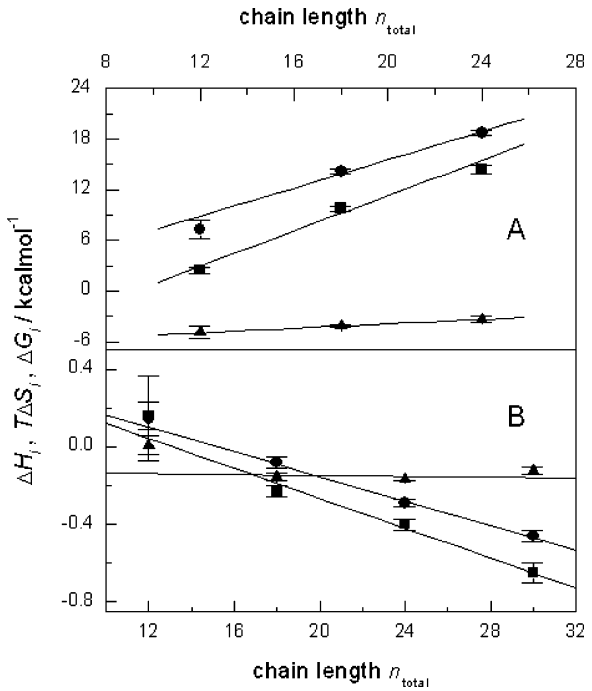

Figure 7. Separation of the peptide binding and peptide folding thermodynamics. (A) Binding parameters (without folding) of peptides of different length. (B) Folding parameters (per amino acid residue) as a function of peptide length. (■) enthalpy ΔH°_i; (●) entropy contribution $T\Delta S^\circ_i$; (▲) Gibbs free energy ΔG°_i.

by the hydrophobic effect; the large gain in entropy upon release of hydration water more than compensates the negative entropies of the aforementioned processes.

We have succeeded in separating the binding reaction proper from the conformational change. This was possible by the synthesis of peptide analogues with D-amino acid substitutions. Figure 6 shows a smooth variation of the thermodynamic parameters of a given peptide (pep-12, pep-18, pep-24) and its D,D analogues with $\Delta\beta$(aa). A clear distinction was found between long (pep-18, pep-24) and short peptides (pep-12). For pep-18 and pep-24 the all-L species exhibits the largest increase in β-structure upon membrane binding but has the smallest endothermic heat of reaction. As D,D substitutions are inserted, $\Delta\beta$-(aa) decreases whereas the heat of reaction increases (negative slope, Figure 6 top panel). In contrast, for the short peptide pep-12 the heat of reaction *increases* with increasing $\Delta\beta$(aa) (positive slope, Figure 6). Corresponding results are found for ΔG° and $T\Delta S^\circ$ (cf. Figure 6). The figure then demonstrates a clear influence of the peptide chain length on binding and folding.

The intercepts of the straight lines in Figure 6 with the *y*-axis report the thermodynamic parameters of the binding process proper as no conformational change is involved (i.e., $\Delta\beta(aa) = 0$). Figure 7A summarizes the chain length dependence of these parameters. The Gibbs free energy of binding, ΔG°_{bind}, shows a moderate increase from −4.8 kcal/mol for pep-12 to −3.2 kcal/mol for pep-24. The initial binding step is thus more favorable for short than for long peptides. As the total free energy ranges between −4.7 (pep-12) to −6.9 kcal/mol (pep-30) the analysis shows that binding without structural change makes the exclusive (pep-12) or a major (pep-18, -24, -30) contribution to the measured thermodynamic parameters.

The slopes of the regression lines in Figure 6 yield the thermodynamic parameters (per residue) of the random coil ⇆ β-structure transition. They are summarized in Figure 7B. For long peptides ($18 \le n \le 30$) the Gibbs free energy of folding, ΔG°_β, is about −0.12 to −0.16 kcal/mol per residue. As a total of ∼14 (in pep-18) to ∼25 (in pep-30) residues undergo this transition, formation of β-structure contributes significantly to the membrane binding process. This parallels the behavior of amphipathic antibacterial peptides where helix-formation leads to negative ΔG°_α and hence to a larger binding affinity.[34]

The corresponding analysis can also be performed for the enthalpy and the entropy term. Figure 7A demonstrates that the enthalpy ΔH°_{bind} is always positive and increases with the chain length. The adverse effect of ΔH°_{bind} is compensated by the positive entropy term $T\Delta S^\circ_{bind}$, which changes almost in parallel with ΔH°_{bind}. For each chain length investigated the association of the $(KIGAKI)_n$ peptides with the membrane is driven by entropy.

A different picture is obtained for the folding process (7B). ΔH°_β and $T\Delta S^\circ_\beta$ change in parallel from positive to negative values such that ΔG°_β is slightly positive for pep-12 but negative for $n_{total} \ge 18$. For the largest peptide measured, pep-30, one finds $\Delta H^\circ_\beta = -0.65$ kcal/mol per residue. This value approaches $\Delta H^\circ_\alpha = -0.74$ kcal/mol per residue established for the membrane induced coil ⇆ helix transition.[34]

The ITC experiments also provide insight into the temperature dependence of ΔG°_{bind} and ΔG°_β. The *binding* enthalpy, ΔH°_{bind}, is *endothermic* for all peptides (Figure 7A) and the binding affinity hence increases at higher temperatures. In contrast, the *folding* enthalpy is *exothermic* for peptides with $n \ge 18$, and less β-structure will develop at higher temperatures. As a consequence of the opposite signs of ΔH°_{bind} and ΔH°_β an increase in temperature leads to better membrane binding but also to a destabilization of β-structure for long KIGAKI peptides.

Concluding Remarks

We have chemically synthesized $(KIGAKI)_x$ peptides of different chain lengths and have investigated their membrane-binding characteristics. A minimum chain length of $n = 7$ amino acids is required to observe binding and detect conformational changes with CD spectroscopy. For peptides with a chain length

of $8 \leq n \leq 30$ a complete thermodynamic characterization was obtained with ITC measurements. Membrane-binding requires an anionic surface, and all bound peptides show an increased β-structure content compared to their conformation in solution. The change in β-content, Δf_β, from solution to membrane exhibits a sigmoidal dependence on the chain length. A separation of peptide binding from peptide folding was possible by synthesizing $(KIGAKI)_n$ analogues with D,D substitutions. For short peptides with $n = 12$, β-structure formation has a positive free energy of $\Delta G^\circ_\beta = 0.08$ kcal mol^{-1} per residue and counteracts binding. For long chains with $n \leq 18$, ΔG°_β is negative with -0.15 kcal mol^{-1} per residue and facilitates membrane binding. ΔH°_β is exothermic with -0.2 to -0.6 kcal/mol per residue supporting folding, whereas $T\Delta S^\circ_\beta$ is negative and inhibits folding. In contrast, the binding step proper is an endothermic reaction ($\Delta H^\circ_{bind} > 0$) and is driven exclusively by entropy ($T\Delta S^\circ_{bind} > 0$). The large positive entropy together with the large negative heat capacity suggests a prominent role of hydrophobic interactions in binding and peptide aggregation.

As initially mentioned, β-sheets in proteins are generally shorter than 10 residues.[2] If our results are interpreted in a more general perspective, the β-sheet folding reaction in proteins would not contribute to a stabilization of protein structure as $\Delta G^\circ_\beta > 0$ for $n \leq 12$. On the other hand, β-sheets in amyloid fibrils are probably longer than 10 residues,[44] and β-structure formation would contribute significantly to fibril stability. Our results then suggest differences in the folding thermodynamics of native and aggregated protein structures.

Materials and Methods

1-Palmitoyl-2-oleoyl-*sn*-glycero-3-phosphoethanolamine (POPE), 1-palmitoyl-2-oleoyl-*sn*-glycero-3-phosphoglycerol (POPG), and 1,2-dioleoyl-*sn*-glycero-3-phosphoethanolamine-*N*-[methoxy (polyethylene glycol)-2000] (mPEG 2000 POPE) were purchased from Avanti Polar Lipids (Alabaster, AL). All other chemicals were purchased at highest purity from various sources.

All peptides were synthesized using the Fmoc (*N*-(9-fluorenyl)-methoxycarbonyl) chemistry on an Applied Biosystems model 433A peptide synthesizer. The crude peptides were purified by reversed phase high performance liquid chromatography (HPLC). Purity was proven by HPLC and mass spectrometry. Peptide concentration in all experiments was determined by absorbance at 280 nm using an extinction coefficient of $\epsilon = 5500$ M^{-1} cm^{-1} for Trp.

Preparation of Lipid Vesicles. Small unilamellar vesicles (SUV) of ~30 nm diameter were prepared as follows. Defined amounts of lipid were dissolved in chloroform and were dried first with a stream of N_2 and then over night under high vacuum. The second and third lipid for the ternary lipid mixtures was added to the dried film in chloroform solution and treated as before. Subsequently, buffer solution was added to the lipid film, and the mixture was vortexed extensively. The lipid dispersion was sonicated with a G112SP1 Special Ultrasonic Cleaner (Laboratory Supplies CO., Inc.) until a clear solution was obtained. To prevent vesicle aggregation all small unilamellar vesicles (SUVs) contained 5 mol % of 1,2-dioleoyl-*sn*-glycero-3-phosphoethanolamine-*N*-[methoxy(polyethylene glycol)-2000] (mPEG 2000 POPE).

Circular Dichroism Spectroscopy. Circular dichroism (CD) measurements were performed with a Jasco J-720 spectropolarimeter. Spectra were recorded at room temperature from 250 to 198 nm, with a resolution of 0.5 nm, response time of 2 s, bandwidth of 1 nm, scan speed of 20 nm/min, and 6 accumulations. CD samples were prepared by adjusting the peptide concentration to 50 μM or 75 μM in 2.5 mM cacodylate buffer at pH 7.4. Aliquots of a 25 mM 45/50/5 POPE/POPG/mPEG (mol %) 2000 POPE SUV dispersion in the same buffer were added to the peptide solution. A control spectrum of pure buffer solution was subtracted from all samples.

Isothermal Titration Calorimetry. Isothermal titration calorimetry (ITC) was performed with a VP ITC instrument (Microcal, Northampton, MA). All measurements were made at 25 °C in buffer (25 mM Tris/HCl, 50 mM NaCl, pH 7.4). Buffer solutions were freshly prepared. The sample cell contained the peptide solution at a concentration of 25−50 μM. Lipid vesicles were prepared in the same buffer (lipid concentration varied from 5 to 25 mM) and injected into the peptide solution in 10 μL aliquots. As a control, lipid vesicles were injected into pure buffer containing no peptide.

Acknowledgment. We thank Sebastian Meier and André Ziegler for carefully proofreading the manuscript. This work was supported by the Swiss National Science Foundation grant no. 3100-107793.

JA077231R

(44) Tycko, R. *Q. Rev. Biophys.* **2006**, *39*, 1−55.